Journal of Organometallic Chemistry, 414 (1991) 11–22
Elsevier Sequoia S.A., Lausanne
JOM 21725

A change of the bonding mode of the alumohydride group in biscyclopentadienylhydrido REM complexes: from heterometallic to homometallic hydrides. Crystal and molecular structures of $[(\eta^5\text{-}C_5H_5)_2Yb(\mu_3\text{-}H)]_2[(\mu_2\text{-}H)AlH_2 \cdot N(C_2H_5)_3]_2 \cdot C_6H_6$, $[(\eta^5\text{-}C_5H_5)_2Lu(\mu_2\text{-}H)]_2[(\mu_2\text{-}H)_2AlH \cdot N(C_2H_5)_3]_2 \cdot C_6H_6$ and $[(\eta^5\text{-}C_5H_5)_2Lu]_3(\mu_2\text{-}H)_2(\mu_3\text{-}H)$

Sergei Ya. Knjazhanskij, Boris M. Bulychev*, Oksana K. Kireeva
Department of Chemistry, Moscow State University, 119899 Moscow (USSR)

Vitalij K. Belsky
L.Ya. Karpov Physico-Chemical Research Institute, 117120 Moscow (USSR)

and Grigorii L. Soloveichik *
Institute of Chemical Physics, Academy of Sciences of the USSR, 142432 Chernogolovka (USSR)

(Received January 20th, 1991)

Abstract

Slight variations of the experimental conditions result in inclusion of non-coordinated benzene molecules into the structures of lutetium and ytterbium alumohydride complexes bringing about resistance to X-ray irradiation in contrast what is found in the benzene-free lutetium complex. X-ray structural determinations of $[(\eta^5\text{-}C_5H_5)_2Yb(\mu_3\text{-}H)]_2[(\mu_2\text{-}H)AlH_2 \cdot N(C_2H_5)_3]_2 \cdot C_6H_6$ (I) (monoclinic crystals: $a = 13.307(2)$, $b = 15.538(2)$, $c = 14.075(2)$ Å, $\gamma = 134.53(1)°$, space group $P2_1/a$, $Z = 4$) and $[(\eta^5\text{-}C_5H_5)_2Lu(\mu_2\text{-}H)]_2[(\mu_2\text{-}H)_2AlH \cdot N(C_2H_5)_3]_2 \cdot C_6H_6$ (II) (monoclinic crystals: $a = 11.339(2)$, $b = 13.300(2)$, $c = 14.061(2)$ Å, $\gamma = 102.28(1)°$, space group $P2_1/b$, $z = 4$) revealed that the former has a classical structure of the adduct between $[Cp_2Ln(\mu\text{-}H)]_2$ and triethylamine with both two μ_3- and μ_2-bridging hydrogens. REM of II is additionally coordinated with one more hydrogen thus increasing its coordination number to 10 with concomitant weakening of the bonding between the dimeric lutetiecene and alane. In excess of triethylamine, complex II decomposes to yield a mixture of $[Cp_2Lu(\mu\text{-}H) \cdot NEt_3]_2$ (VI) and $[(\eta^5\text{-}C_5H_5)_2Lu]_3(\mu_2\text{-}H)_2(\mu_3\text{-}H)$ (VII). The latter, according to X-ray data (hexagonal crystals: $a = 16.193(3)$, $c = 10.640(1)$ Å, space group $P3_12_12$, $Z = 3$), has a triangular metal core with central μ_3-hydrogen.

Introduction

Recently, we described how X-ray irradiation (Mo-K_α) [1] induced an unusual solid-state rearrangement of the monocrystal of the dimeric 18e lutetiecene alumohydride into the 14e monomer, following equation 1.

$$[Cp_2Lu(\mu_3\text{-}H)]_2[(\mu_2\text{-}H)AlH_2\cdot NEt_3]_2 \xrightarrow{h\nu} 2\ Cp_2Lu(\mu_2\text{-}H)AlH_3\cdot NEt_3 \qquad (1)$$

The irradiation is needed only to initiate the transition, which can proceed further even in its absence. Other effectors, such as pressure, temperature or irradiation of polycrystalline samples, do not generate the monomer [2]. The complex $[Cp_2Lu(\mu_3\text{-}H)]_2[(\mu_2\text{-}H)AlH_2\cdot OC_4H_8]_2$ [1] and the structural analogue of the lutetiecene complex, the compound $[Cp_2Y(\mu_3\text{-}H)]_2[(\mu_2\text{-}H)AlH_2\cdot NEt_3]_2$ [3] are also unaffected by irradiation. However, strictly speaking, the latter is not a complete analogue of the lutetium complex because yttrium does not have *f*-electrons. Therefore, in order to deepen our understanding of the driving forces of reaction 1, we have prepared ytterbiecene alumohydride solvated by triethylamine and, in addition, have investigated the complex formation in the system $Cp_2LuCl\text{-}LiAlH_4\text{-}NEt_3\text{-}C_6H_6\text{-}Et_2O$.

Results and discussion

The interaction of biscyclopentadienyl ytterbium and lutetium chlorides with $LiAlH_4$ in the medium ether–benzene–triethylamine brings about precipitation of LiCl followed by crystallization of orange (M = Yb (I)) or colourless (M = Lu (II)) complexes of the same formula, $Cp_2LnAlH_4\cdot NEt_3\cdot 0.5C_6H_6$, equation 2.

$$Cp_2LnCl + LiAlH_4 + NEt_3 \xrightarrow{C_6H_6,\ Et_2O} Cp_2LnAlH_4\cdot NEt_3\cdot 0.5C_6H_6 + LiCl \qquad (2)$$

Table 1

Summary of crystal data for complexes $[(\eta^5\text{-}C_5H_5)_2Yb(\mu_3\text{-}H)]_2[(\mu_2\text{-}H)AlH_2\cdot N(C_2H_5)_3]_2\cdot C_6H_6$ (I), $[(\eta^5\text{-}C_5H_5)_2Lu(\mu_2\text{-}H)]_2[(\mu_2\text{-}H)_2AlH\cdot N(C_2H_5)_3]_2\cdot C_6H_6$ (II) and $[(\eta^5\text{-}C_5H_5)_2Lu]_3(\mu_2\text{-}H)_2(\mu_3\text{-}H)$ (VII)

	I	II	VII
Formula	$C_{19}H_{32}NAlYb$	$C_{19}H_{32}NAlLu$	$C_{30}H_{33}Lu_3$
Fw	474.49	476.42	918.51
Crystal system	monoclinic	monoclinic	hexagonal
Space group	$P2_1/a$	$P2_1/b$	$P3_12_12$
a, Å	13.307(2)	11.339(2)	16.193(3)
b, Å	15.538(2)	13.300(2)	16.193(3)
c, Å	14.075(2)	14.061(2)	10.640(1)
γ, deg	134.53(1)	102.28(1)	120
V, Å^3	2074.7(6)	2072.1(7)	2415.6(8)
Z	4	4	3
d_{calc}, g/cm^3	1.52	1.53	1.89
Diffractometer	Nicolet $P3$	Syntex $P\bar{1}$	Syntex $P\bar{1}$
μ_{Mo}, cm^{-1}	47.0	50.4	96.0
$2\theta_{max}$, °	48	45	50
Ref. refined	2278	1848	923
$I > n(I)$, n	3	3	3
Method of solution	Patterson	Patterson	Patterson
Program	SHELXTL	SHELXTL	SHELXTL
Absorp. correction	included	not included	included
R	0.038	0.076	0.034
R_w	0.040	0.086	0.036

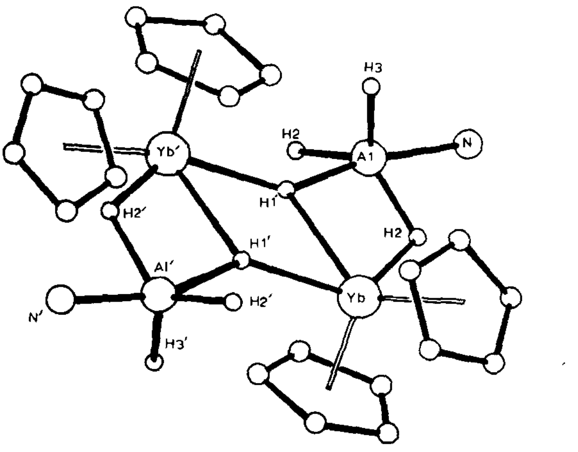

Fig. 1. Molecular structure of the complex $[(\eta^5\text{-}C_5H_5)_2Yb(\mu_3\text{-}H)]_2[(\mu_2\text{-}H)AlH_2 \cdot N(C_2H_5)_3]_2 \cdot C_6H_6$.

It should be noted that under these conditions $LiAlH_4$ does not reduce Yb^{III} to Yb^{II}. The only difference between our procedure and those reported elsewhere [1,2] is the higher ratio $NEt_3 : Ln$ (equal to 10 : 1 and 100–150 : 1) for complexes I and II respectively (not more than 5 : 1 in ref. 1). This, however, is sufficient for the preparation of compounds with non-coordinated benzene. Their structure is profoundly altered as a result and II, in particular, differs significantly from $[Cp_2Lu(\mu_3\text{-}H)]_2[(\mu_2\text{-}H)AlH_2 \cdot NEt_3]_2$ (IIa) reported earlier [1].

In contrast to IIa, both I and II are resistant to Mo-K_α irradiation and their reflections do not change in the course of the experiment. The experimental data indicate that despite close similarity of atomic radii of Yb and Lu, complexes I and II are not isostructural although their elementary cell volumes are practically equal (Table 1). Both compounds are made of dimeric molecules $[Cp_2LnAlH_4 \cdot NEt_3]_2$ (Figs. 1 and 2), the layers of which are separated by layers of non-coordinated benzene molecules. The distance between their layers is close to the sum of their Van-der-Waals radii.

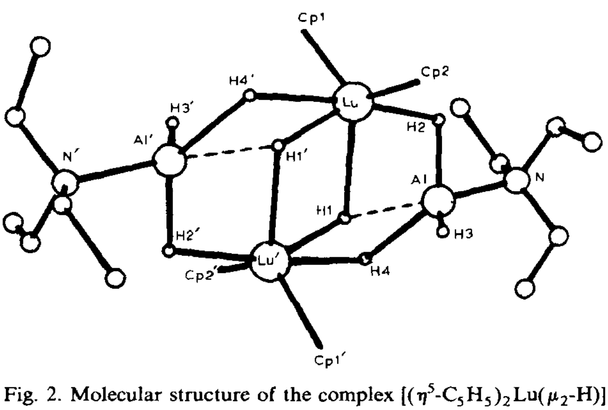

Fig. 2. Molecular structure of the complex $[(\eta^5\text{-}C_5H_5)_2Lu(\mu_2\text{-}H)]_2[(\mu_2\text{-}H)_2AlH \cdot N(C_2H_5)_3]_2 \cdot C_6H_6$.

Table 2

General interatomic distances (Å) and valent angles (deg) for $[CpLnAlH_4 \cdot NEt_3]_2 \cdot C_6H_6$ (Ln = Yb (I), Lu (II))

Bond	I	II	Angle	I	II
M–Cp1	2.33	2.29	Cp1MCp2	127.9	128.4
M–Cp2	2.32	2.29	H1MH1′	57(2)	56(4)
M···M′	3.623(1)	3.613(1)	H1MH2	70(2)	86(4)
M···Al	3.260(2)	3.26(1)	H1′MH4′	–	51(4)
M′···Al	3.728(3)	4.09(1)	AlMM′	72(2)	80(4)
M–H1	2.09(5)	2.35(9)	MAlM′	68(2)	57(4)
M–H1′	2.04(5)	1.73(9)	H1AlH2	73(2)	97(4)
M–H2	2.15(5)	2.57(9)	H1AlH3	92(2)	51(4)
M–H4′	–	2.61(9)	H1AlH4	83(2)	49(4)
$M–C_{av}$	2.60	2.59	H1AlN	166(2)	167(4)
Al–H1	2.31(5)	2.69(9)	H2AlH3	125(2)	118(4)
Al–H2	1.61(5)	1.75(9)	H2AlH4	113(2)	129(4)
Al–H3	1.50(5)	1.32(9)	H2AlN	93(2)	77(4)
Al–H4	1.58(5)	1.96(9)	H3AlH4	117(2)	73(4)
Al–N	2.108(8)	2.13(3)	H3AlN	99(2)	121(4)
$N–C_{av}$	1.51(3)	1.53(4)	MH1M′	122(1)	123(2)
$(C–C)_{av}^{Et}$	1.54(4)	1.49(6)	MH2Al	119(1)	96(2)
			MH4′Al′	–	124(2)

A mutual arrangement of non-hydrogen atoms in I and II does not differ significantly and is much the same as in $[Cp_2Y(\mu_3\text{-}H)]_2[(\mu_2\text{-}H)AlH_2 \cdot NEt_3]_2$ (III) [3] and $[Cp_2Y(\mu_3\text{-}H)]_2[(\mu_2\text{-}H)AlH_2 \cdot THF]_2$ (IV) [4]. It should be mentioned in passing that the distances M···M and M···Al decrease progressively with decreasing covalent radius of the metal (Tables 2 and 3). The parameters of the wedge-like sandwiches Cp_2M in I and II are also similar.

The cyclopentadienyl rings in both complexes are in an eclipsed conformation maximising separation of bridging hydrides from the rings. At the same time interatomic distances and bond angles involving bridging hydrogens are so unlike in I–IV that one can speak about a change of the bonding mode of the alumohydride

Table 3

Main interatomic distances (Å) for dimeric alumohydride complexes of biscyclopentadienyllantanides and Y

Complexes	M···M	M···Al	$M–\mu_3$-H	$M–\mu_2$-H	$Al–\mu_3$-H	$Al–\mu_2$-H	Al–L	Ref.
$(Cp_2YbAlH_4 \cdot NEt_3)_2 \cdot C_6H_6$ (I)	3.62 3.73	3.26	2.1	2.2	2.3	1.6	2.11	[a]
$(Cp_2LuAlH_4 \cdot NEt_3)_2 \cdot C_6H_6$ (II)	3.61 4.09	3.26 2.4	1.7	2.6	2.7	1.7 2.0	2.13	[a]
$(Cp_2YAlH_4 \cdot NEt_3)_2$ (III)	3.70	3.31 4.11	–	–	–	–	2.13	[3]
$(Cp_2YAlH_4 \cdot THF)_2$ (IV)	3.75	3.24 4.00	2.2 2.3	2.2	2.0	1.6	1.97	[4]
$[(C_5H_4^tBu)_2SmAlH_4 \cdot THF]_2$ (V)	4.23	3.25 3.28	2.4	2.2	1.8	1.6	2.00	[5]

[a] This paper.

moiety. In ytterbium complex I, the system of hydride bonds is identical, in general, to that in yttrium complexes III and IV [3,4] and may be formulated as $[Cp_2Ln(\mu_3\text{-}H)]_2[(\mu_2\text{-}H)AlH_2 \cdot L]_2$. The main structural component motive in molecule I (as in other alumohydride complexes $(Cp_2LnAlH_4 \cdot L)$ is the dimer

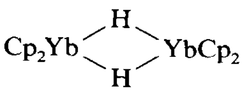

coordinated by two triethylaminalane molecules through μ_2- and μ_3-hydrogens (Fig. 1). In complex I, ytterbium is bonded with three hydrogens which are slightly, by ~ 0.1 Å, out of the bisector plane of both the wedge-like sandwiches Cp_2Yb. Aluminium and nitrogen atoms lie also in this plane.

The metallacycle YbH_2Al is not planar: the dihedral angle along the H1–H2 axis is 13.6°. The Yb–H bond lengths in YbH_2Yb are somewhat lower than those observed in III [3] and $[(C_5H_4^tBu)_2Sm(\mu_3\text{-}H)]_2[(\mu_2\text{-}H)_2AlH \cdot THF]_2$ (V) [5] (Table 3), whereas the bond Al–(μ_3-H1) is significantly longer (by 0.3–0.5 Å) than that in complexes III–V, the bond Al–(μ_2-H2) showing a minor change. It thus can be concluded that in I there is some bond strengthening in the metallacycle YbH_2Yb and some weakening of the bonding between $(Cp_2YbH)_2$ and alane. This tendency is even more clear on going from I to II.

Although heavy atoms of the metallacycle LuH_2Lu in II do not change their mutual arrangement this becomes asymmetric and leaves the bisector plane of the wedge-like sandwiches Cp_2Lu (the angle between the Cp_2Lu and LuH_2Lu planes is 59.9°, while the corresponding angle in complex I is 92.0°). This increases strongly the interatomic distance Al–(μ_3-H1) up to 2.7 Å. Therefore, this bond should be treated as "secondary", rather than covalent. Such a bonding of aluminium with bridging chlorides in the dimer $(Cp_2Y(\mu_2\text{-}Cl)]_2$ ($d(Al \cdots Cl) = 3.01$ Å) has been previously found in the complex $\{[Cp_2Y(\mu_2\text{-}Cl)]_2(\mu_2\text{-}H)_2AlH \cdot Et_2O\}_n$ [6]. The elongation of the Lu–(μ_3-H1) bond in complex II is accompanied by the elongation of the Lu–(μ_3-H2) bond in the bridge Lu–H–Al (Table 2). Unlike what is seen in complexes I and III, two hydrogens of alane are now bonded with Lu (Fig. 2). The same is observed in the samarium complex V. However, in contrast to the latter, the bond distances Al–(μ_2-H) in II are markedly increased (Table 3). To this end, there is only one terminal hydrogen at Al in II while there are four hydrides in the first coordination sphere of Lu bringing about, as in V [5], a formal 20e configuration. Since four hydrogens probably cannot be positioned in the bisector plane of the wedge-like sandwich Cp_2M, they partially (complex V) or completely (complex II) leave the plane thus contradicting the MO formalism [7]. One can overcome this discrepancy by assuming that AO of REM contributing most to the $1a_1$, $2a_1$ and b_2 hydridic orbitals of the wedge-like sandwich Cp_2M are diffusive in nature and, hence, can overlap with the $1s$ hydrogen orbitals located out of the bisector plane.

The coordination polyhedron of Al in I and II, as in the majority of similar compounds [8], is a distorted trigonal bipyramide, the axial sites being occupied by nitrogen and hydrogen of the metallacycle LnH_2Ln. It should be pointed out that the distortion takes place in all heterometallic hydridic complexes of Al and transition metals while it is highest for the complexes containing a tridentate alumohydride group.

The analysis of the metal–hydrogen bond distances in complexes I–V (Table 3) suggests that the strength of the bond between alane and $(Cp^{\star}{}_2LnH)_2$ decreases with decreasing size of Ln, being the lowest in complex II in which the bonds Lu–(μ_2-H) and Al–(μ_3-H) may be considered as secondary. Obviously, under certain conditions $AlH_3 \cdot NEt_3$ may dissociate. In fact, on increasing the amount of the amine up to $[NEt_3]:[Lu] = 250:1$ and diluting the solutions ($[Cp_2LuCl] < 0.1$ *M*), a mixture of crystals of two compounds in the ratio 1 : 1 is formed in the system $Cp_2LuCl–LiAlH_4–NEt_3–C_6H_6–Et_2O$. The crystals do not contain aluminium and their shape is different. The IR spectrum of the mixture is a superposition of two spectra without the bands from terminal M–H bonds (1600–1900 cm^{-1}). Bands at 1360, 955 and 675 cm^{-1}, by analogy with the spectrum of $[Cp_2Lu(\mu_2\text{-H}) \cdot THF]_2$ [9], were assigned to vibrations of the metal–hydride bonds in $[Cp_2Lu(\mu_2\text{-H}) \cdot NEt_3]_2$ (VI). Bands at 1215, 820 and 700 cm^{-1} are typical of hydridic compounds of the type $[(Cp^{\star}{}_2LnH)_3X]^-[M \cdot THF_n]^+$ [10–12] and may be assigned to the trinuclear complex. Structure was established by X-ray crystallography. The crystals are composed of neutral trimeric molecules $[(\eta^5\text{-}C_5H_5)_2Lu]_3(\mu_2\text{-H})_2(\mu_3\text{-H})$ (VII) (Figure 3), but the structure differs drastically from that of the ionic trimer $\{[(\eta^5\text{-}C_5H_5)_2Er(\mu_2\text{-H})]_3(\mu_3\text{-H})\}^-[Li(THF)_4]^+$ (VIII) [10] and the ring compound $[(Me_2C_5H_3)_2YH]_3$ (IX) [13].

The metal core of VII, as of IX, is almost an ideal triangle, but the bond lengths Lu ··· Lu are 0.4–0.5 Å shorter than those designated Y ··· Y in IX while the difference in metal covalent radii is only 0.06 Å. This, in our opinion, is strong evidence for the rationalization of IX as a trimer in which the fragments $Cp_2''Y$ are triply (μ_2-H) bridged (hydrogens were not localized in ref. 13). The location of a μ_3-bridging hydrogen in VII, practically in the centre of the Lu_3 triangle, is the reason for decrease of the Lu ··· Lu distances. Structural differences in trimers VII and IX probably arise from the cyclopentadienyl ligands differing in bulk: in complex IX the ligand methyl moieties shield effectively the loose ring trimer while the tight trimer of VII with μ_3-H atom is effectively shielded by the usual C_5H_5-rings.

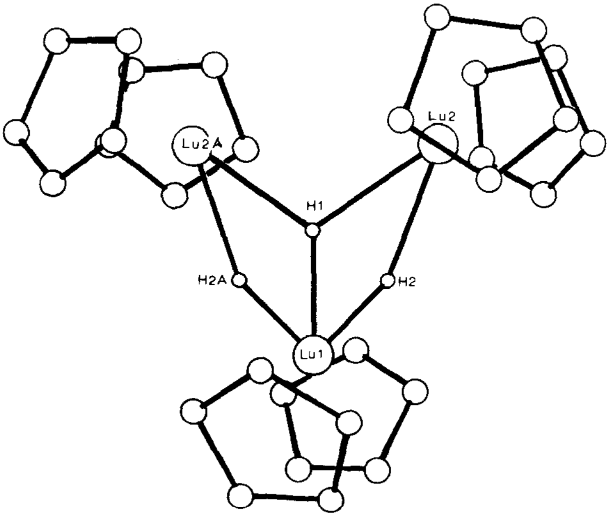

Fig. 3. Molecular structure of the complex $[(\eta^5\text{-}C_5H_5)_2Lu]_3(\mu_2\text{-H})_2(\mu_3\text{-H})$.

As seen in Figure 3, lutetium atoms in VII are nonequivalent: the central one (Lu1) is coordinated by three hydrogens (coordination number 9), while the edge ones are coordinated by two (c.n. 8). At the same time the distance Lu1 ··· Lu2 in VII is much shorter (taking into account the difference in covalent radii) than the Er ··· Er distance in the trinuclear complex VIII with central μ_3-hydrogen (3.68 Å) [10], while the distance Lu2 ··· Lu2A is almost equal to it. Usually, in complexes with Ln c.n. of 9, the bond lengths Ln–C_{Cp} and Ln–X are 0.06–0.15 Å longer than those in complexes with Ln c.n. of 8 (for example, the bond length Y–C_{Cp} in $[Cp''_2YH \cdot THF]_2$ is equal to 2.69 Å [13], in $[Cp''_2YH]_3$ to 2.63 A [13]; the bond length Gd–Br in $[Cp_2GdBr]_n$ is equal to 3.02 Å [14,15], but in $[Cp_2GdBr]_2$ to 2.88 Å [15]). This rule does not hold in VII, since the bond length Lu1–CpI is 0.04–0.12 Å shorter than Lu2–CpII and Lu2–CpIII (Table 4) and, besides, is the shortest among those reported for hydridic REM complexes. The shortening of the bond length Lu1–H1 (1.86 Å) and Lu1–H2 (1.56 Å) in comparison with Lu2–H2 and Lu2–H1 (2.13 and 2.22 Å, respectively) should also be mentioned. Even when the low precision of determination of hydrogen coordinates is taken into account, the short contact Lu1–H1 is worth mentioning. In fact, while Lu2–H distances are quite common for lanthanidecene hydrides (for example, 1.98 and 2.13 Å in $[Cp_2LuH \cdot THF]_2$ [12]), the bond lengths Lu1–H are even shorter than in $[(SiMe_3)_2C_5H_3]_2$-$ScBH_4$ ($R_{cov.Sc} = 1.42$ Å, d(Sc–H) = 2.03 Å [16]). It is possible that all these unique structural features are due to the unusual arrangement of hydrogen ligands in VII. The values of bond angles (Table 4) and the extremely short H ··· H contact (1.31 Å) suggest that these atoms interact with the adjacent $1a_1$ and b_2 orbitals of Lu2 rather than with $1a_1$ and $2a_1$ orbitals as usually occurs in the fragments

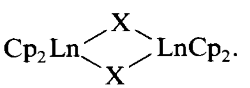

Besides, one cannot rule out completely the contribution from the ionic moiety $[Cp_2Lu]_2^+[Cp_2LuH_3]^-$.

Although trimers of type VII have not been described in the literature, a closely related pattern of the REM bonding through μ_2- and μ_3-halides was observed in the zig-zag ribbon-like polymers $[Cp_2GdBr]_n$ [14,15], $[Cp_2DyCl]_n$ [14] and the tetramer $[Cp_2GdCl]_4$ [17]. In the latter, as in VII, the Cp-rings at internal metal centres with

Table 4

General interatomic distances (Å) and valent angles (deg) for $(Cp_2Lu)_3(\mu_2\text{-}H)_2(\mu_3\text{-}H)$ (VII)

Lu1–Cp*1	2.29	Cp*1LuCp*1′	126.7
(Lu1–C)$_{av}$	2.55	Cp*2LuCp*2′	124.4
Lu2–Cp*2	2.33	Lu2Lu1Lu2A	61.1(1)
Lu2–Cp*2′	2.41	Lu1Lu2Lu2A	59.5(1)
(Lu2–C)$_{av}$	2.60; 2.66	H1Lu1H2	44.1(5)
Lu1 ··· Lu2	3.607(2)	H2Lu1H2A	88.3(5)
Lu2 ··· Lu2A	3.667(4)	H1Lu2H2	35.1(5)
Lu1–H1	1.86(5)	Lu1H1Lu2	124.2(5)
Lu1–H2	1.56(5)	Lu2H1Lu2A	111.6(5)
Lu2–H1	2.22(5)	Lu1H2Lu2	155.6(5)
Lu2–H2	2.13(5)		

c.n. = 9 are in an eclipsed conformation, while the edge ones with c.n. = 8 are staggered. Therefore, the majority of complexes Cp_2LnX may be considered as oligomers $(Cp_2LnX)_n$ with the limiting values $n = 2$ and ∞. The degree of oligomerization is evidently dictated by the relative sizes of Ln and X, as well as by the bulkiness of Cp★-ligands, leading to $n = 3$ in the case of VII.

The uniqueness of the reaction leading to VII is that this non-solvated compound is formed in a large excess of a strong donor ligand, i.e. triethylamine. Decomposition of II according to equation 3 is not typical of alumohydride REM complexes with C_5H_5- ligands, but it is well understood in view of the structure of the starting complex and our observations [18,19], where similar dissociation of solvated alane from $[(C_5H_3^tBu_2)_2LuH]_2[AlH_3 \cdot OEt_2]_2$ was observed in the ether-pentane medium.

$$(Cp_2LuH)_2(AlH_3 \cdot NEt_3)_2 \longrightarrow (Cp_2LuH)_2 + 2AlH_3 \cdot NEt_3 \quad (3)$$

The unsolvated, coordinatively unsaturated dimer $(Cp_2LuH)_2$, being a strong Lewis acid, is not stable in the presence of a strong base transforming into amine solvate VI or the oligomer $(Cp_2LuH)_n$ as is observed in complexes $[Cp_2DyCl]_n$ or $[Cp_2GdCl]_4$. The second channel of the reaction is provided by the relatively low coordinating ability of NEt_3 with respect to the dimer $(Cp_2LuH)_2$, attributed to the large bulk of the former. Crystallization of trimer VII from the reaction mixture is indicative of a higher stability of this oligomeric lutetiecene hydride because of the optimal geometrical correspondence of the hydride ligand and the wedge-like sandwich Cp_2Lu. Since the unsolvated intermediate $\{Cp_2LuH\}$ does not seem probable in reaction 3, the formation of VII probably occurs on dissociation of oligomers with "n" being in the series 6, 12, etc.

To conclude, the unique behaviour of complex VII under X-ray irradiation should be emphasized. As a result, colourless crystals of VII gradually became bright blue. The colour change under Cu-K_α irradiation is by a factor of 2–3 times faster than that under Mo-K_α irradiation. In contrast to IIa, however, complex VII does not undergo any structural transition (the unit cell parameters do not change after irradiation), although in both cases there are variations in physical properties of the samples (monomerization of IIa and an increase in the colour intensity of VII) which are observed even after exposure.

At the same time complexes I and II are resistant to irradiation and transitions of type 1 are not observed. The reason becomes evident on comparison of the cell

Table 5

The crystallographic characteristics of biscyclopentadienylalumohydride complexes of Y, Yb and Lu

Complex	a, Å	b, Å	c, Å	γ, deg	V, Å^3	d, g/cm^3 [a]
$(Cp_2YbAlH_4 \cdot NEt_3)_2 \cdot C_6H_6$ (I)	13.31	15.54	14.07	134.5	2075	1.52 (1.53) [a]
$(Cp_2LuAlH_4 \cdot NEt_3)_2 \cdot C_6H_6$ (II)	11.34	13.30	14.06	102.3	2072	1.53
$(Cp_2LuAlH_4 \cdot NEt_3)_2$ (IIa)	11.35	13.34	14.20	102.0	2103	1.38
$Cp_2LuHAlH_3 \cdot NEt_3$ (IIb)	13.28	9.70	14.10	94.2	1811	1.60
$(Cp_2YAlH_4 \cdot NEt_3)_2$ (III)	11.38	13.39	14.16	102.0	2110	1.12 (1.39)
$(Cp_2YAlH_4 \cdot THF)_2$ (IV)	8.75	11.04	16.45	95.6	1581	1.36 (1.72)
$(Cp_2LuAlH_4 \cdot THF)_2$ (IVa)	8.73	11.06	16.42	95.6	1579	1.72

[a] In parentheses; approximate values calculated by changing Y to Lu in the structures of the complexes. References are given in the text.

parameters and the densities of the biscyclopentadienylalumohydride Y, Yb and Lu complexes (Table 5). Complexes I and II have closely similar cell parameters and are practically isomorphous to IIa. Their X-ray density, however, is very similar to that of monomer IIb because of the presence of non-coordinated benzene molecules. The latter, evidently, occupy the vacancies (which are found in IIa) in I and II, thus transforming a loose, compressible structure into a tight, and hence stable, one. The density of complexes $[Cp_2Ln(\mu_3\text{-H})]_2[(\mu_2\text{-H})AlH_2 \cdot THF]_2$ (Ln = Y (IV) [4], Lu (IVa) [1]), $Cp_2YAlH_4 \cdot 0.5Et_2O$ [3] and $(Cp_2Y)_2Cl(AlH_4 \cdot NEt_3)$ [6], in contrast to that of IIa, is high (Table 5) and they are resistant to transition of type 1. At the same time yttrium complex III, the analogue of IIa, also has a low density structure but transition 1 does not occur [3]. The nature of the metal is likely to play a role in the reaction 1.

Experimental

X-Ray structural determinations of crystal I, II and VII were carried out in sealed glass capillaries. The conditions and crystallographic parameters are given in

Table 6

Atomic coordinates ($\times 10^4$, hydrogen atoms $\times 10^3$) and equivalent isotropic displacement coefficients $[(C_5H_5)_2YbAlH_4 \cdot NEt_3]_2 \cdot C_6H_6$ (I)

Atom	*x*	*y*	*z*	B_{eq}
Yb	5708(1)	4866(1)	6024(1)	39(1)
Al	8370(3)	7125(3)	4753(2)	48(2)
C(1)	5844(13)	5069(12)	7869(8)	72(12)
C(2)	6842(13)	6217(13)	7558(8)	79(11)
C(3)	6196(14)	6521(11)	7083(7)	76(11)
C(4)	4751(13)	5503(12)	7122(7)	72(11)
C(5)	4547(13)	4615(10)	7595(7)	69(9)
C(6)	4427(12)	2646(9)	6158(8)	62(8)
C(7)	4699(12)	2907(10)	5206(9)	65(9)
C(8)	6135(13)	3704(10)	5058(8)	60(10)
C(9)	6769(11)	3952(10)	5925(7)	64(8)
C(10)	5736(14)	3296(10)	6602(7)	66(11)
N	10538(7)	8290(7)	5047(6)	54(6)
C(11)	11346(23)	8658(21)	4160(15)	68(17)
C(11)A	11359(25)	9561(24)	4650(21)	97(21)
C(12)	11272(15)	9461(13)	3528(11)	111(13)
C(13)	11107(22)	9393(19)	5569(21)	85(17)
C(13)A	10829(30)	8492(25)	6097(16)	87(24)
C(14)	10472(14)	9153(15)	6560(11)	115(13)
C(15)	10797(21)	7625(20)	5650(16)	63(17)
C(15)A	11146(22)	7834(20)	4677(17)	70(17)
C(16)	10557(13)	6667(11)	5146(8)	77(10)
CB(1) [a]	157(17)	66(17)	941(9)	100(16)
CB(2)	452(15)	984(14)	479(13)	106(13)
CB(3)	256(16)	907(14)	−457(17)	104(14)
H(1)	7899	6404	5739	
H(2)	8231	6639	3825	
H(3)	8514	8167	4769	
H(4)	4057	4227	5184	

[a] CB are the carbon atoms of the benzene molecule.

Table 1. The structures were solved by the Patterson method and refined by the least squares method in an anisotropic/isotropic (H atoms) approximation. The hydride hydrogens were localized by difference Fourier synthesis. In complexes I and II, triethylamine α-carbons occupy two sets of random positions with fixed β-carbons corresponding to two different orientations of the ethyl groups, clockwise and counter-clockwise relative to the Al–N axis. Main interatomic distances and bond angles are given in Tables 2–4. Atomic coordinates are in Tables 6–8.

$[Cp_2YbAlH_4 \cdot NEt_3]_2 \cdot C_6H_6$ (I)

To a red solution of Cp_2YbCl (1.63 g, 4.8 mmol) in 200 ml benzene 5 ml NEt_3 (10-fold excess) and 4.8 mmol $LiAlH_4$ in 10 ml ether were added. The mixture became yellow and LiCl precipitated. The solution was filtered and concentrated up to 150 ml. Yellow cubic crystals formed were washed with 100 ml benzene and dried *in vacuo* to yield 1.8 g (88%) of $[Cp_2YbAlH_4 \cdot NE_3]_2 \cdot C_6H_6$. Found: Yb, 36.4; Al, 5.6. $C_{19}H_{32}NYbAl$ calc.: Yb, 36.5; Al, 5.7%.

Table 7

Atomic coordinates ($\times 10^4$, hydrogen atoms $\times 10^3$) and equivalent isotropic displacement coefficients $[(C_5H_5)_2LuAlH_4 \cdot NEt_3]_2 \cdot C_6H_6$ (II)

Atom	x	y	z	B_{eq}
Lu	5135(1)	5843(1)	6020(1)	33(1)
Al	2869(8)	6247(7)	4758(7)	42(3)
C(1)	4495(49)	4236(27)	7118(25)	87(19)
C(2)	3490(37)	4658(34)	7069(26)	80(17)
C(3)	3834(40)	5639(31)	7566(28)	91(19)
C(4)	5020(25)	5778(26)	7763(26)	82(14)
C(5)	5451(28)	4921(29)	7593(23)	55(13)
C(6)	6332(30)	7407(22)	5038(21)	46(11)
C(7)	5868(35)	7846(21)	5936(25)	56(14)
C(8)	6759(29)	7420(24)	6590(23)	52(12)
C(9)	7295(49)	6797(30)	6177(30)	105(21)
C(10)	7127(30)	6771(23)	5194(26)	58(13)
N	1704(25)	7254(18)	5068(21)	51(11)
C(11)	2358(61)	8175(47)	5671(46)	59(24)
C(11)A	2205(85)	8335(43)	4664(49)	75(35)
C(12)	3336(33)	8887(25)	5150(28)	65(13)
C(13)	1301(37)	7689(39)	4140(38)	53(20)
C(13)A	437(57)	6794(59)	4600(78)	72(36)
C(14)	543(45)	6833(40)	3505(36)	103(22)
C(15)	534(64)	6768(76)	5594(71)	90(38)
C(15)A	1590(66)	7299(69)	6095(55)	90(35)
C(16)	866(39)	6327(36)	6579(33)	99(19)
CB(1) [a]	978(38)	543(33)	5499(50)	84(22)
CB(2)	897(47)	635(32)	4536(48)	95(22)
CB(3)	−56(56)	98(38)	4056(33)	96(22)
H(1)	4732	5340	4432	
H(2)	3212	6576	5945	
H(3)	3734	6482	4121	
H(4)	2922	4976	4076	

[a] CB are the carbon atoms of the benzene molecule.

Table 8

Atomic coordinates ($\times 10^4$, hydrogen atoms $\times 10^3$) and equivalent isotropic displacement coefficients $[(\eta^5\text{-}C_5H_5)_2Lu]_3(\mu_2\text{-}H)_2(\mu_3\text{-}H)$ (VII)

Atom	x	y	z	B_{eq}
Lu(1)	4082(1)	4082(1)	0	42(1)
Lu(2)	6483(1)	5519(1)	1164(1)	42(1)
C(1)	2685(34)	3137(41)	1540(46)	96(33)
C(2)	3361(19)	3874(30)	2193(25)	75(21)
C(3)	3413(23)	4682(23)	1744(24)	74(19)
C(4)	2865(30)	4475(28)	774(22)	80(26)
C(5)	2369(21)	3467(29)	727(24)	84(21)
C(6)	7479(45)	4639(49)	1326(43)	134(45)
C(7)	6949(31)	4258(32)	440(52)	102(27)
C(8)	7112(32)	4775(38)	−482(31)	84(26)
C(9)	7845(39)	5711(42)	−283(37)	121(37)
C(10)	8117(30)	5616(50)	1021(50)	230(42)
C(11)	5916(27)	6257(30)	3006(22)	107(30)
C(12)	5811(29)	5414(29)	3455(22)	84(24)
C(13)	6695(24)	5535(24)	3644(22)	79(22)
C(14)	7315(22)	6362(23)	3333(24)	73(18)
C(15)	6950(52)	6876(25)	2949(28)	115(36)
H(1)	5231	5231	0	
H(2)	5084	4459	598	

$[Cp_2LuAlH_4 \cdot NEt_3]_2 \cdot C_6H_6$ (II)

To a yellow suspension of Cp_2LuCl (1.02 g, 3 mmol) in a mixture C_6H_6 (140 ml)–NEt_3 (62 ml) (Lu: $NEt_3 = 1:150$) $LiAlH_4$ (3 mmol) in 6.5 ml ether was added dropwise with vigorous stirring. The suspension was stirred until completely decolorized followed by filtration of LiCl. The solution was concentrate by 1/10. Colourless prisms (0.6 g) were separated after 30 h, washed with benzene and vacuum dried. Found: Lu, 36.7; Al, 5.6. $C_{19}H_{32}NLuAl$ calc.: Lu, 36.7; Al, 5.7%.

$(Cp_2LuH \cdot NEt_3)_2$ (VI) and $(Cp_2LuH)_3$ (VII)

To Cp_2LuCl (0.68 g, 2 mmol) suspended in 200 ml benzene and 70 ml NEt_3 (Lu : $NEt_3 = 1:250$) a solution of $LiAlH_4$ (2 mmol) in 7 ml ether was added dropwise with vigorous stirring and the mixture was stirred for 1 h until decolorized, and precipitation of LiCl followed. After filtration, the solution was allowed to stand for several days to produce a mixture of two differently shaped colourless crystals, mica-like plates and crystals looking like a 18-crown-6 molecule. They were filtered and vacuum dried. Yield 0.6 g. Found: Lu, 48.9; Al, 0.0%. The synthesis is poorly reproducible.

References

1 S.Ya. Knjazhanskij, B.M. Bulychev, V.K. Belsky and G.L. Soloveichik, J. Organomet. Chem., 327 (1987) 173.

2 S.Ya. Knjazhanskij, V.K. Belsky, B.M. Bulychev and G.L. Soloveichik, Metalloorg. Khim., 2 (1989) 345.

3 V.K. Belsky, A.B. Erofeev, B.M. Bulychev and G.L. Soloveichik, J. Organomet. Chem., 365 (1984) 123.

4 V.K. Belsky, B.M. Bulychev, A.B. Erofeev and G.L. Soloveichik, J. Organomet. Chem., 268 (1984) 107.
5 Yu.K. Gun'ko, B.M. Bulychev, A.I. Sizov, V.K. Belsky and G.L. Soloveichik, J. Organomet. Chem., 390 (1990) 153.
6 A.B. Erofeev, B.M. Bulychev, V.K. Belsky and G.L. Soloveichik, J. Organomet. Chem., 335 (1987) 189.
7 J.W. Lauher and R. Hoffmann, J. Am. Chem. Soc., 98 (1976) 1729.
8 B.M. Bulychev, G.L. Soloveichik, V.K. Belsky and A.I. Sizov, Metalloorg. Khim., 2 (1989) 82.
9 W.J. Evans, J.H. Meadows, A.L. Wayda, W.E. Hunter and J.L. Atwood, J. Am. Chem. Soc., 104 (1982) 2008.
10 W.J. Evans, J.H. Meadows, A.L. Wayda, W.E. Hunter and J.L. Atwood, J. Am. Chem. Soc., 104 (1982) 2015.
11 W.J. Evans, J.H. Meadows and T.P. Hanusa, J. Am. Chem. Soc., 106 (1984) 4454.
12 H. Schumann, W. Genthe, E. Hahn, M.B. Hossain and D. van der Helm, J. Organomet. Chem., 299 (1986) 67.
13 W.J. Evans, D.K. Drummond, T.P. Hanusa and R.J. Doedens, Organometallics, 6 (1987) 2279.
14 W. Lamberts and H. Lueken, Inorg. Chim. Acta, 132 (1987) 119.
15 W. Lamberts, h. Lueken and U. Elsenhans, Inorg. Chim. Acta, 121 (1987) 81.
16 M.F. Lappert, A. Singh, J.L. Atwood and W.E. Hunter, J. Chem. Soc., Chem. Commun., (1983) 206.
17 W. Lamberts, B. Hessner and H. Lueken, Inorg. Chim. Acta, 139 (1987) 215.
18 S.Ya. Knjazhanskij, V.K. Belsky, B.M. Bulychev and G.L. Soloveichik, Metalloorg. Khim., 2 (1989) 570.
19 S.Ya. Knjazhanskij, B.M. Bulychev, E.B. Lobkovskii, V.K. Belsky and G.L. Soloveichik, J. Organomet. Chem., (JOM 21975) in press.